



# An artificial intelligence system using machine-learning for automatic detection and classification of dental restorations in panoramic radiography

Ragda Abdalla-Aslan, DMD,<sup>a</sup> Talia Yeshua, PhD,<sup>b</sup> Daniel Kabla, BSc,<sup>c</sup> Isaac Leichter, PhD,<sup>d</sup> and Chen Nadler, DMD, PhD<sup>e</sup>

**Objectives.** The aim of this study was to develop a computer vision algorithm based on artificial intelligence, designed to automatically detect and classify various dental restorations on panoramic radiographs.

**Study Design.** A total of 738 dental restorations in 83 anonymized panoramic images were analyzed. Images were automatically cropped to obtain the region of interest containing maxillary and mandibular alveolar ridges. Subsequently, the restorations were segmented by using a local adaptive threshold. The segmented restorations were classified into 11 categories, and the algorithm was trained to classify them. Numerical features based on the shape and distribution of gray level values extracted by the algorithm were used for classifying the restorations into different categories. Finally, a Cubic Support Vector Machine algorithm with Error-Correcting Output Codes was used with a cross-validation approach for the multiclass classification of the restorations according to these features.

**Results.** The algorithm detected 94.6% of the restorations. Classification eliminated all erroneous marks, and ultimately, 90.5% of the restorations were marked on the image. The overall accuracy of the classification stage in discriminating between the true restoration categories was 93.6%.

**Conclusions.** This machine-learning algorithm demonstrated excellent performance in detecting and classifying dental restorations on panoramic images. (Oral Surg Oral Med Oral Pathol Oral Radiol 2020;130:593–602)

Artificial intelligence (AI) for improving radiologic diagnosis has been widely studied and is rapidly entering clinical use.<sup>1</sup> To improve and facilitate computer-aided diagnosis, models relying on both visual and spatial information are needed to automate image analysis.<sup>2,3</sup> Computer output is used to improve the accuracy and consistency of the radiologic diagnosis.<sup>1,4</sup> An AI algorithm generally consists of several steps, including image processing, feature analysis, and data classification, with the use of machine-learning tools.

Panoramic imaging is one of the most widely used radiographic examinations because of its broad demonstration of most of the oromaxillofacial structures on a single image, with minimal patient discomfort and low radiation effective dose (14.2–24.3  $\mu$ Sv).<sup>5,6</sup> Most often, it demonstrates pathoses in the dentition and in the jaws; some of the pathoses may be incidental

findings not encountered during clinical examination. The prevalence of incidental findings in panoramic images of young patients undergoing orthodontic treatment was found to be 8.7%, and these findings included idiopathic sclerosis, mucosal thickening, and periapical lesions.<sup>7</sup> Moreover, Rushton et al. showed that in the majority of panoramic radiographs (95.4%–96.9%), there are significant dental and nondental findings, including cystic lesions, diseases of the maxillary antrum, temporomandibular joint diseases, and soft tissue calcifications.<sup>8</sup> They also found that experienced dental radiologists diagnose these findings, especially the nondental findings, more often compared with general dentists. Although international guidelines suggest that findings on panoramic radiographs should be entered into the patient's clinical record,<sup>9</sup> there is currently no universal practice of generating a specific radiographic report. AI technology may facilitate the production of such a report, further improving patient management and communication.

Most studies dealing with computer processing of panoramic radiographs refer to the development of algorithms, which identify only teeth, without

<sup>a</sup>Researcher, Attending Physician, Department of Oral and Maxillofacial Surgery, Rambam Health Care Campus, Haifa, Israel.

<sup>b</sup>Lecturer, Department of Applied Physics/Electro-optics Engineering, The Jerusalem College of Technology, Jerusalem, Israel.

<sup>c</sup>Department of Electrical and Electronics Engineering, The Jerusalem College of Technology, Jerusalem, Israel.

<sup>d</sup>Professor Emeritus, Department of Applied Physics/Electro-optics Engineering, The Jerusalem College of Technology, Jerusalem, Israel.

<sup>e</sup>Lecturer, Oral Maxillofacial Imaging Unit, Oral Medicine Department, the Hebrew University, Hadassah School of Dental Medicine, Ein Kerem, Hadassah Medical Center Jerusalem, Israel.

Received for publication Jan 8, 2020; returned for revision Apr 28, 2020; accepted for publication May 22, 2020.

© 2020 Published by Elsevier Inc.

2212-4403/\$-see front matter

<https://doi.org/10.1016/j.oooo.2020.05.012>

## Statement of Clinical Relevance

A computer vision algorithm based on supervised machine learning demonstrated excellent performance in detecting and classifying various dental restorations on panoramic images. Possible useful applications include patient diagnosis and treatment planning, students' education, and forensic dentistry.

detecting dental restorations. Patanachai et al. proposed a tooth segmentation technique for panoramic images based on wavelet transformation.<sup>10</sup> Poonsri et al. proposed a fully automatic algorithm to segment teeth.<sup>11</sup> Their algorithm consisted of 3 steps: tooth area identification, template matching of single and double rooted teeth, and tooth area segmentation. However, its accuracy was less than 50% because of tooth inclination and low contrast between teeth and surrounding tissues. In another approach to automatically segment teeth on a panoramic radiograph, Lira et al. proposed texture recognition based on supervised learning techniques.<sup>12</sup> Those authors developed a Bayesian classifier that could distinguish between pixels inside and outside teeth, but the classifier was applied only to 4 panoramic radiographs, resulting in accuracy of 81.3%.<sup>12</sup> An algorithm to detect only third molars was developed by Amer et al., who used the basic functions of image processing and the relative order in which these teeth appear on the panoramic radiograph.<sup>13</sup> An algorithm for tooth segmentation and characterization of teeth with or without caries was described by Oliviera et al., but this algorithm did not detect the precise location of caries.<sup>14</sup>

Machine-learning is a subset of AI that provides systems with the ability to automatically learn and improve performance from experience, without being explicitly programmed.<sup>15</sup> Its primary aim is to allow the computer to learn automatically without human intervention or assistance and to adjust the algorithm accordingly. Machine-learning models can provide a concise representation of complicated real-world phenomena and enable predictions of future events from present observations.<sup>16</sup> Machine-learning algorithms use a training data set, from which the machine is then able to learn and draw conclusions to make decisions on its own. The algorithm outcomes are then compared with a tested set of actual data to quantify its accuracy. As the data in the training sets grow and the number of testing repetitions increases akin to experiential learning, the machine-learning algorithm becomes more accurate and more predictive.<sup>17</sup> In the supervised machine-learning applied in this study, the algorithm analyzes the given patterns in the training data set, and on the basis of the results, creates a model for automatically classifying the new data set.

Computerized algorithms for the detection and classification of dental restorations, as well as early detection of oral pathologic findings on panoramic radiographs, have not been previously reported. Automatic detection and classification of dental restorations is the initial stage that enables the detection of abnormalities, such as periodontal bone loss and dental caries, which often occur adjacent to existing dental restorations. In addition, this stage is required to map

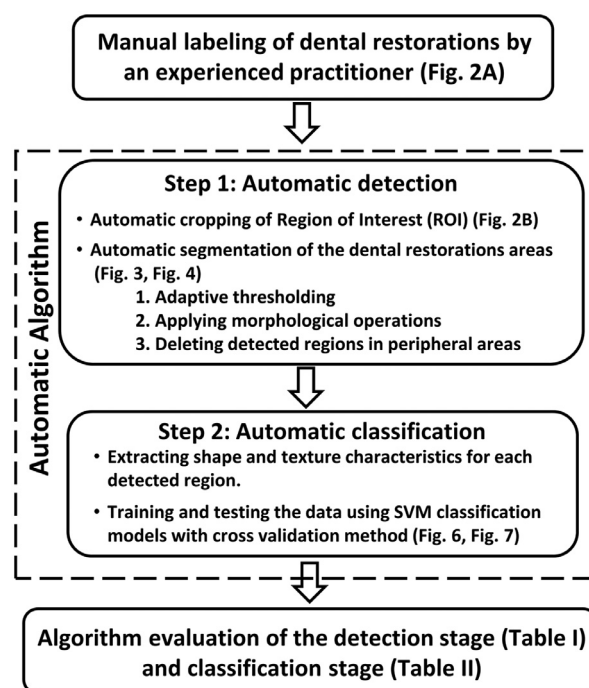
dental restorations and separate them from other incidental, nondental maxillofacial diseases.

The aim of this study was to develop a machine-learning algorithm designed to automatically detect and classify dental restorations on panoramic radiographs as an initial step toward automatic detection of maxillofacial abnormalities.

## MATERIALS AND METHODS

### Study layout

The study was composed of 3 parts as shown in **Figure 1**: (1) manual labeling of the dental restorations in the panoramic images, which served as the “ground truth”; (2) automatic algorithm development, which consisted of 2 steps: automatic detection (step 1) involving the development of an algorithm for detecting dental restorations, and automatic classification (step 2) involving the development of an algorithm for classifying the restorations into categories; and (3) evaluation of the performance of the algorithm with respect to the detection and classification steps and comparing it with the “ground truth.”



**Fig. 1.** A study flow-chart for the algorithm development for the detection and classification of dental restorations in panoramic radiography. Dental restorations were initially manually identified and labeled by an experienced practitioner (“ground truth”). The automatic algorithm development consisted of 2 steps; step 1 included automatic detection, and step 2 included automatic classification of the restorations. Algorithm performance was evaluated for both the detection and classification stages and compared with the “ground truth.”

## Study data set

Eighty-three anonymized panoramic images, including 738 dental restorations, were randomly selected as the index cases from the archives of the Imaging Center of the Department of Oral Medicine, Sedation, and Imaging at the Hebrew University Hadassah School of Dental Medicine (Jerusalem, Israel). The patient cohort consisted of 40 males and 43 females (age 16–97 years; average  $41.8 \pm 20.6$  years). Panoramic images were obtained by using an Orthopantomograph OP200 machine (Instrumentarium Dental, Milwaukee, WI) with an image size of  $2734 \times 1422$  pixels, and viewed by using Scanora diagnostic software IAM version 5.11.13923 (Soredex, Chicago, IL). The study was approved by the Hadassah institutional review board (HMO-0190-18).

## Manual labeling of dental restorations

An oral medicine specialist (R.A.A.) with experience in maxillofacial imaging evaluated the panoramic images and manually identified and labeled the existing dental restorations according to 6 detection categories (DCs): amalgam filling (AF); composite filling (CF); crown (CRW); dental implant (DI); root canal treatment (RCT); and core (CO). Whenever more than 1 DC was observed for a single tooth, the specialist labeled all relevant DCs as one entity. For example, a tooth with a dental implant and a crown was labeled as DI+CRW, and a tooth that had undergone root canal treatment with placement of a core and a crown was labeled as RCT+CO+CRW, as shown in Figure 2A.

## Automatic algorithm development

**Step 1: Automatic detection of dental restorations.** The algorithm was developed in the Matlab environment by using image processing and machine learning toolboxes. The algorithm included 2 steps, as shown in Figure 1: automatic detection of the dental restorations (step 1) and automatic classification of the detected regions (step 2). Before step 1, the panoramic image was automatically cropped to obtain only the region of interest (ROI) containing the maxillary and mandibular alveolar ridges. The borders of the ROI were experimentally calculated to include the alveolar ridge in all of the data sets. In the vertical axis, the algorithm set the upper limit of the cropping region at 18% from the upper border of the image, and the lower limit was set at 24% above the lower border. In the horizontal axis, the ROI was cropped symmetrically, that is, 17% from both horizontal borders (Figure 2B). This was performed to significantly reduce the running time of the algorithm because the cropped ROI was 38.5% of the size of the original panoramic image.

For the detection of dental restorations, the algorithm used a gray level thresholding method. The

panoramic radiographic image is composed of different gray level values, with mostly higher values for restorations compared with teeth and surrounding tissues. Consequently, the detection of restorations was performed by gray level thresholding so that all the pixels with gray level values higher than the threshold would be attributed to restorations. However, allotting a single global threshold value for the entire radiograph was not appropriate because of the inhomogeneity of the gray levels in the image. Instead, an adaptive approach was applied, making use of different threshold values in different regions of the image. In this approach, the threshold gray level value for each pixel was automatically calculated by considering only the gray levels of the pixels in a local window around the desired pixel, rather than the gray levels of the entire ROI. The local threshold was calculated by using a Gaussian filter that weights the gray level of each pixel in the local window in accordance with a Gaussian bell-curve that is calibrated by using the relative distance from the pixel in the center of the window. Local windows of different sizes were examined,<sup>18</sup> and the size of the local window that yielded the optimal segmentation of the restorations was about 6% of the length and 6% of the width of the ROI ( $101 \times 51$  pixels). Figure 3 illustrates the detection process in a cropped portion of a panoramic image. Figure 3A displays a magnified region of the image with several restorations. Figure 3B displays a binary image in which the restorations were detected by using a single global threshold value calculated by the Otsu method.<sup>19</sup> Figure 3C displays a binary image in which the restorations were detected by using a Gaussian adaptive threshold. This figure demonstrates that although the edge of the root canal treatment appears darker than the space between the first premolar composite filling and the crown next to it, the adaptive threshold detected the whole root canal treatment and separated the composite filling and the crown.

Next, several morphologic operations were required to improve the results of initial detection by the adaptive threshold. A morphologic opening was performed for separating adjacent restorations that were erroneously identified as a single region. A rectangular structuring element of  $3 \times 10$  pixels, which gave the optimal opening, was used. The detection results after the morphologic opening are shown in Figure 3D, where the composite filling of the first molar is separated from the crown. However, this operation also tended to disconnect regions that ought to be considered a single region, and as a result, the root canal treatment edge in Figure 3D was disrupted. The closing operation that was then performed, by using a smaller structuring element of  $3 \times 3$  pixels to connect erroneously separated

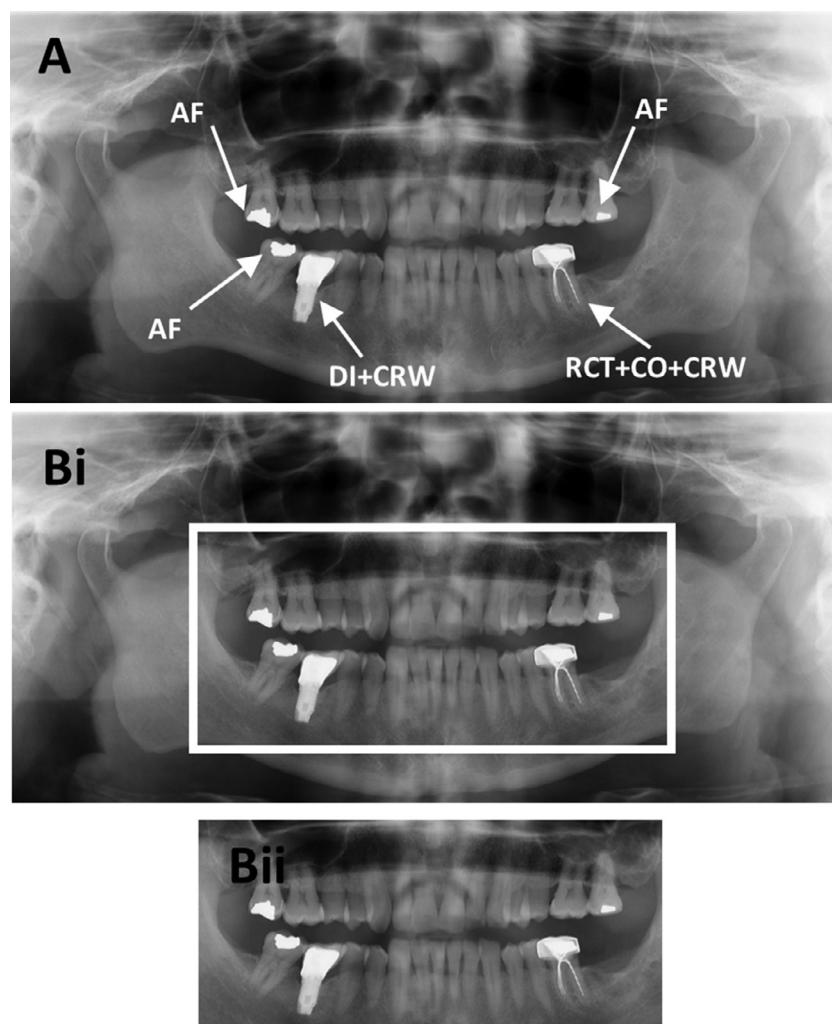


Fig. 2. (A) Manual labeling of dental restorations. An example of an index case showing manual markings of 5 restorations of 3 types (AF, DI+CRW, and RCT+CO+CRW) by an oral medicine specialist with experience in maxillofacial imaging. (B) Automatic cropping of the region of interest (ROI). An example of the index case showing panoramic image before (Bi) and after (Bii) cropping of the ROI, which includes the dentition in both arches and its surrounding maxillary and mandibular alveolar bone. AF, amalgam filling; CO, core; CRW, crown; DI, dental implant.

regions, connected the 2 parts of the root canal treatment, as shown in Figure 3 E. At this stage, the detection results also included regions smaller than the size of a standard dental restoration, so the algorithm then erased all the detected regions containing less than 450 pixels. Finally, a hole-filling operation was performed to include all internal pixels belonging to the detected regions. Figure 3 F shows the detection results after erasure of the small detected regions and the hole-filling operation.

The results of the algorithm at this point showed that most of the detected regions close to the edges of the ROI did not represent restorations. However, the apical areas of root canal treatments and dental implants were located quite near the edges of the ROI. Therefore, to remove only the erroneously detected regions close to

the edges, all regions with a center of mass located at the top 15% of the ROI and at the bottom 12% of the ROI were removed.

The final detection stage of the algorithm could result in the detection of (1) regions with a single restoration; (2) regions with multiple restorations of different DCs; and (3) regions that were falsely marked. Figure 4 shows an example of the automatic detection stage.

*Step 2: Automatic classification of the detected regions.* The second step of the algorithm was to classify all the detected regions into classification categories (CCs). For the classification step, 11 CCs were defined, including 8 CCs of dental restorations and 3 CCs of false (erroneous) marks, as depicted in Figure 5.



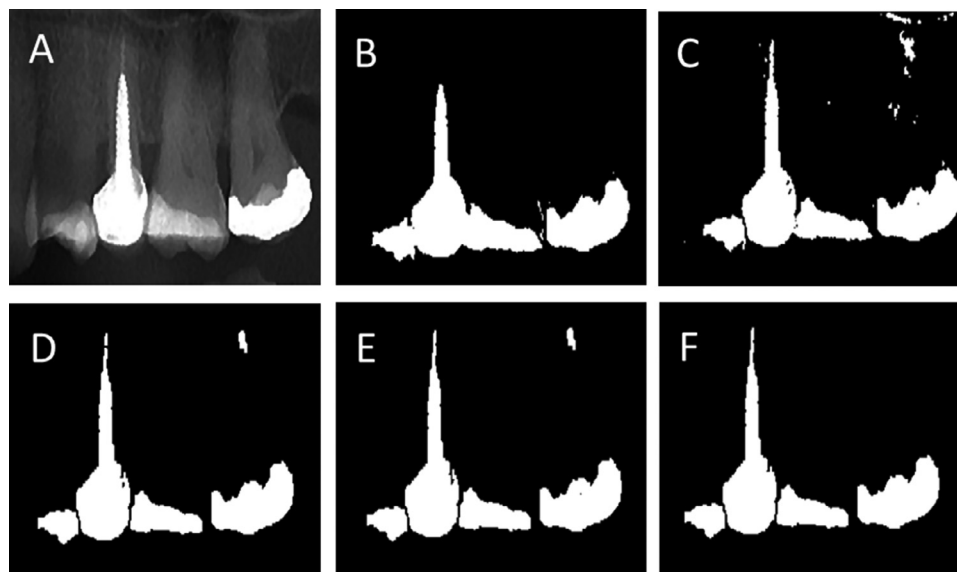


Fig. 3. The automatic detection process. (A) A magnified region of a panoramic image. (B) A binary detection image obtained by using a single global threshold. (C) A binary detection image obtained by using an adaptive threshold with a Gaussian filter, leading to detection of the root canal filling and separation of the first premolar composite filling from the crown. (D) The adaptive detection results after the opening operation, leading not only to separation of the composite filling in the first molar but also to discontinuity within the root canal treatment. (E) The adaptive detection results after the closing operation, leading to connection of the 2 parts of the root canal treatment. (F) The final detection results after erasure of the small regions and the hole-filling operation.



Fig. 4. Automatic detection of regions containing dental restorations. An example of the index case showing a panoramic image with computerized markings (in red) of the 5 dental restorations that were detected.

Four CCs of dental restorations included a simple (single) type of restoration: (1) AF; (2) CF; (3) CRW; or (4) DI. Three additional CCs included entities with combined restorations: (5) RCT+CO; (6) RCT+CO+CRW; or (7) DI+CRW. Furthermore, dental restorations in neighboring teeth, as visualized on the panoramic image as one region, were also categorized as a single CC with combined restorations (8) (MULTI). The 3 CCs of false marking errors consisted of tissues that appeared brighter than their surroundings and were not dental restorations. These included: (9) overlap between neighboring teeth, (10) tooth enamel, and (11) other false markings, such as cortical plates (e.g.,

external oblique line) and pulp stones. Other types of dental restorations, including steel crowns and retentive pins, were not included in this preliminary study because they are not commonly encountered. In addition, panoramic images that included dental restorations together with dentures, bars, or orthodontic appliances were excluded from the study.

Classification of the dental restorations was carried out by extracting the numerical features that described the shape and the texture of each detected region. The shape characteristics included the area, perimeter, circularity, solidity, area-equivalent diameter, and orientation of the detected region. The texture






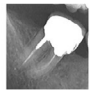

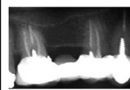
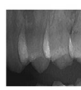

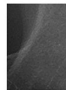
Simple (single) type of restoration	1. AF	2. CF	3. CRW	4. DI
				
Combined restorations	5. RCT+CO	6. RCT+CO+CRW	7. DI+CRW	8. MULTI
				
False marking errors	9. Overlap	10. Tooth Enamel	11. Other False	
				

Fig. 5. The classification categories. Examples of the 11 classification categories for the detected regions in our database, composed of simple (single) type of restoration, combined restorations and false marking errors. *AF*, amalgam filling; *CF*, composite filling; *CO*, core; *CRW*, crown; *DI*, dental implant; *RCT*, root canal treatment.

characteristics included the average gray level value, standard deviation of the gray level, smoothness, and statistical entropy of the gray level values in the detected region. Additional texture characteristics were used for calculating the spatial allocation of the gray levels and not only their global distribution. These properties included contrast, correlation, homogeneity, and energy, and were computed by using the Gray Level Co-occurrence Matrix.<sup>20</sup>

The machine-learning classification algorithm used the data set of regions, which had been manually labeled for studying the unique characteristics of each of the 11 CCs, and created models for optimal discrimination of the CCs. In the training step, the learning algorithm compared the classification output for the various regions with the corresponding manual labels

and modified the model to minimize errors. In the testing step, the algorithm was blinded to the manual labels of another data set of detected regions that was used, while it classified the detected regions by the models that had been created in the training step.

The cross-validation method was applied for evaluating the classification performance of the algorithm<sup>16,21,22</sup> (Figure 6). To this end, all the detected regions were randomly divided into 5 groups. Training was carried out by using 4 groups from the database, and classification was tested by using the fifth group. This process was repeated 5 times, alternating the testing group and the training groups each time.

Finally, support vector machine-learning (SVM) algorithms were used for creating different models of classification. The SVM algorithm is a binary classifier,

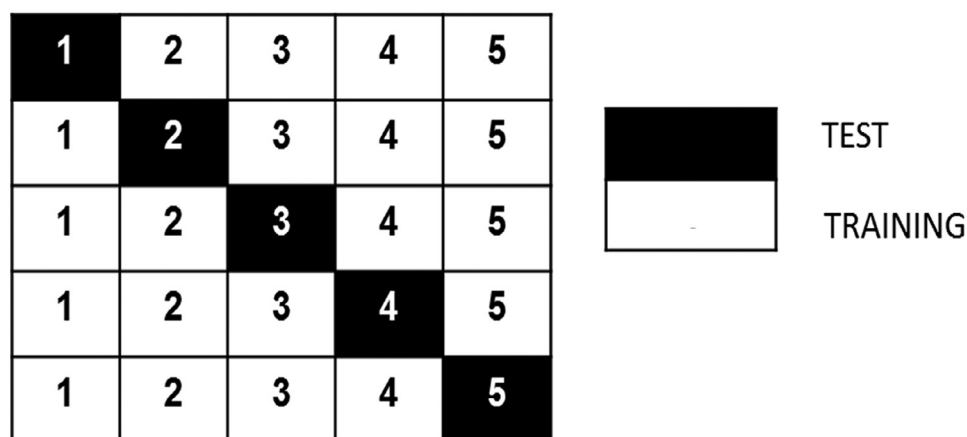


Fig. 6. Illustration of the cross-validation classification process. All detected regions were arbitrarily divided into 5 groups. Four groups were used for training the algorithm, whereas the fifth was used to test the machine-learning process. This stage was repeated 5 times, with all 5 groups.

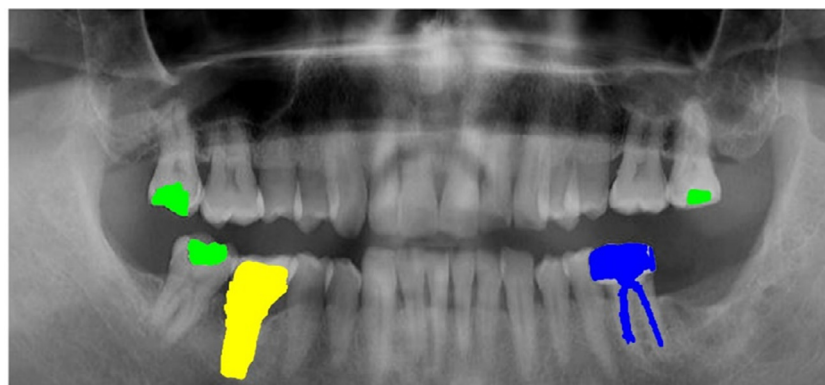


Fig. 7. Automatic classification of the dental restorations. An example of the index case showing a panoramic image with computerized markings of three categories marked in different colors—green, AF; blue, RCT+CO+CRW; and yellow, DI+CRW.

which is basically designed to calculate a plane separation between 2 groups. The calculated plane can be a linear plane (linear SVM), a parabolic plane (quadratic SVM), or a third-degree polynomial plane (cubic SVM). Because the classification of the detected restorations into various categories is a multiclass problem, SVM was used along with Error-Correcting Output Codes,<sup>23</sup> which constitute a meta-method combining many binary classifiers to solve the multiclass problem. For our data classification, SVM along with Error-Correcting Output Codes produced better classification results compared with other classifiers, such as decision tree and naive Bayes, which can handle multiclass problems directly. After classification of the diverse CCs, they were marked on the panoramic image in different colors (Figure 7).

#### Algorithm evaluation of the detection and classification steps

The performance of the automatic detection stage was evaluated on the basis of detection sensitivity, which was calculated as the number of restorations automatically detected by the machine-learning algorithm out of the number of restorations manually labeled by the oral medicine specialist (the “ground truth”) for each type of restoration and for the total of all restorations.

The performance of the automatic classification stage was evaluated by calculating the sensitivity, specificity, positive predictive value (PPV), negative predictive value (NPV), and accuracy of the algorithm for each CC with respect to the ground truth.

## RESULTS

### Detection stage

In some cases, when a region identified by the algorithm comprised restorations of several DCs, not all the individual restorations were detected. In such cases, only the detected restorations could be analyzed at the

classification step. Therefore, when evaluating the detection performance, we analyzed the detection sensitivity of each restoration separately. For example, in a region comprising a dental implant with a crown, the sensitivity detection for each DC was evaluated separately because sometimes only the crown was detected. In such a case, only the detected crown could be classified in the classification step.

In the detection stage, the algorithm identified 1305 regions as containing dental restorations. Of these, 431 regions included either a single restoration or a combination of restorations (altogether 698 restorations were detected), and the remaining 874 detected regions were erroneous (false) markings. The detection sensitivity of the different DCs ranged from 83.1% to 100%, with an overall sensitivity of 94.6% (698 restorations were detected of the 738 that were manually labeled). The detection sensitivities were highest for amalgam fillings and crowns and lowest for composite fillings and root canal treatments (Table I).

### Classification stage

The Cubic-SVM machine-learning algorithm created the model that provided the best categorization outcome compared with the manual labeling. The diagnostic performance of the classification step was analyzed separately for each CC as shown in Table II. The algorithm classified most of the restorations with high sensitivity rates of 96% to 100%, but CF (80.9%) and RCT+CO (74.3%) had lower sensitivity. The other metrics of detection (specificity, PPV, NPV, and accuracy) all exceeded 90% for each category.

During the classification stage, all the erroneous markings were classified as such (sensitivity of 100%), and as a result, on the final image, the algorithm did not mistake any erroneous marks for restorations. In total, 18 detected regions, including 30 restorations, were incorrectly classified as erroneous marks,

**Table I.** Performance of the automatic detection stage

Type of restoration category (acronym)	Number of restorations manually labeled	Number of restorations automatically detected	Detection sensitivity
Amalgam filling (AF)	197	197	100%
Composite filling (CF)	77	64	83.1%
Crown (CRW)	182	182	100%
Dental implant (DI)	52	49	94.2%
Root canal treatment (RCT)	137	114	83.2%
Core (CO)	93	92	98.9%
<b>Total</b>	<b>738</b>	<b>698</b>	<b>94.6%</b>

AF, amalgam filling; CF, composite filling; CO, core; CRW, crown; DI, dental implant; RCT, root canal treatment.

**Table II.** Performance of the automatic classification stage

	AF	CF	CRW	DI	RCT+CO	RCT+CO+CRW	DI+CRW	MULTI	All erroneous marks
Sensitivity	100%	80.9%	100%	97.7%	74.3%	96.0%	100%	97.2%	100%
Specificity	99.6%	99.8%	100%	99.9%	100%	100%	100%	99.9%	95.6%
PPV	96.8%	96.5%	100%	97.7%	100%	100%	100%	98.6%	97.9%
NPV	100%	99.0%	100%	99.9%	99.3%	99.8%	100%	99.8%	100%
Accuracy	99.6%	98.9%	100%	99.9%	99.3%	99.8%	100%	99.8%	98.6%

AF, amalgam filling; CF, composite filling; CO, core; CRW, crown; DI, dental implant; NPV, negative predictive value; PPV, positive predictive value; RCT, root canal treatment.

producing a PPV of 97.9%. As a result, the algorithm finally correctly identified and marked 90.5% of the restorations (668 of 738) on the images. The overall accuracy of the classification step to discriminate between the true restoration categories (without including the CCs of the erroneous marks) was 93.6%.

## DISCUSSION

Although panoramic images are very widely used, they pose some technical challenges for AI. These include distortions as well as variability of the gray level values because of projections of anatomic structures outside the focal plane, which cause ghost images overlapping the desirable images.<sup>24</sup>

In this study, we developed a machine-learning algorithm for automatic detection and classification of dental restorations on panoramic radiographs as an initial step to enable the detection of dental and maxillofacial abnormalities, such as caries, periodontal diseases, and other bone lesions. This goal is challenging because the quality of the panoramic image is frequently suboptimal. Image contrast depends on selecting the correct peak kilovoltage (kVp), and panoramic radiographs sometimes have distortions, which are highly sensitive to head positioning within the machine. The panoramic images used in this study were produced by a single unit. We intend to test the developed algorithm in subsequent studies to assess the robustness in different imaging centers and dental offices resulting in a variety of image quality.

In this study, we chose 11 classification categories that describe the most commonly encountered restorations. Then, for simplicity of manual labeling and for training the algorithm, these were divided into simple (single) types of restorations or combinations of different types. Other types of restorations and dental treatment that were not included in this preliminary study, such as steel crowns, pins, and radiolucent composite fillings, will be assessed in future work.

The machine-learning system showed a high level of diagnostic performance compared with the manual labeling of the oral medicine specialist, with 94.6% overall sensitivity in the detection stage and 93.6% overall accuracy in the classification stage. In the detection step, the algorithm used advanced tools of image processing and computer vision tools for detecting dental restorations. The algorithm uses an adaptive gray level thresholding approach, making use of different threshold values in different regions of the image. This method performs well with regions where there is a sharp gray level boundary dividing objects of different densities. Therefore, of the 6 DCs, the detection sensitivities of amalgam fillings, crowns, dental implants, and cores were greater than 94%. The detection of composite fillings and root canal treatments was more complicated because the gray level values of composite fillings are similar to those of normal teeth and because root canal fillings are presented on the image as very narrow structures. As a result, the detection rates of both were lower (83.1% and 83.2%, respectively).



In the classification step, 11 CCs had to be defined because some of the detected regions comprised multiple restorations of different DCs. The CCs included 4 single restoration categories, 4 combinations of multiple restorations, and 3 categories of erroneous marks. The machine-learning algorithm was trained to classify the CCs by using characteristic features describing the shape and texture of the restorations in each category.

The sensitivity values in the detection of amalgam fillings, crowns, and dental implants with or without crowns were very high, similar to the detection phase, but these values for composite fillings and root canal treatment were lower. Part of the reason may be that composite fillings and root canal treatments with cores were detected with a lower sensitivity, and the missed restorations were never classified. In addition, these 2 categories were classified in some of the cases as erroneous marks because of their relatively low gray level values.

The algorithm-generated sensitivity of the erroneous marks was 100%, and therefore, although they were detected in the detection step, the final algorithm did not mark them on the image. The high classification rate of erroneous marks may have resulted from the large training group (874 erroneously detected regions classified into 3 categories) that was used to teach the algorithm which of the detected regions were not restorations. However, the algorithm also wrongly classified 30 restorations as erroneous marks.

Although the performance of the algorithm produced excellent detection and classification rates, this pilot investigation had a few limitations. The study included images from one panoramic machine and the cropping of the images was performed by experimental calculations. Further algorithm development is required to create a completely automated method for various panoramic units, without human operator intervention to set the initial parameters. This will provide a more comprehensive test for the accuracy of classifying image objects. As stated before, this will be assessed in subsequent studies.

Other limitations of the study were that some categories included small numbers of restorations (composite fillings and dental implants), which may have impaired the training process. Furthermore, not all types of restorations and dental treatments were included in the study. We plan to address them in future research.

In addition, restorations that were not correctly identified in the detection step of the algorithm did not reach the classification step. The use of deep learning algorithms, which merge the detection and classification steps, could overcome the last 2 limitations. However, satisfactory detection of the contour of the various restorations by using deep learning will require much larger data sets of restorations in each category

and accurate manual marking and labeling of each restoration. This is in line with previous research recognizing that considerable amount of development is needed to reach 100% accuracy for successful automatic analysis.<sup>2</sup>

Dental restorations detected by automated computer processing are valuable for various applications that can promote the patient's health. Because the analysis of the information in the images relies on the dentist's experience and visual perception, the computerized detection and classification of dental restorations can serve to verify and substantiate the diagnostic confidence of the dentist. Conveying this information directly to the patient may improve patient–clinician communication by providing an accurate, automated representation of the current dental status to assist in individual oral health promotion programs.<sup>25</sup> In addition, it provides objective information, which may help increase a patient's motivation to receive treatment, increase confidence in the dentist's diagnosis, and reduce apprehension about dental treatments.<sup>26</sup> This detailed description may also aid the prescriber in the description of radiologic findings, including the patient's restorative status.

Similar computer algorithms can be used in radiology education, where students can exercise their detection abilities to understand patient information regarding restorations, saving time and personnel.<sup>27</sup> Last, the ability to create an automated characterization of dental restorations is part of the dental biometric. This is important in forensic dentistry and can aid in subject identification as part of the Automated Dental Identification System.<sup>28,29</sup>

## CONCLUSIONS

This study described a pilot machine-learning algorithm developed to detect and classify dental restorations on panoramic images. The algorithm performed well in both the detection and classification steps. Further research is needed to improve the algorithm's performance by including all available restorations types and for assessing its generalizability and validity in various panoramic machines.

## REFERENCES

1. Shiraishi J, Li Q, Appelbaum D, Doi K. Computer-aided diagnosis and artificial intelligence in clinical imaging. *Semin Nucl Med.* 2011;41:449-462.
2. Benn DK. Automatic analysis of radiographic images: II. Software implementation and testing on bitewing radiographs. *Dentomaxillofac Radiol.* 1991;20:193-199.
3. Benn DK. Automatic analysis of radiographic images: I. Theoretical considerations. *Dentomaxillofac Radiol.* 1991;20:187-192.
4. Doi K. Computer-aided diagnosis in medical imaging: Historical review, current status and future potential. *Comput Med Imaging Graph.* 2007;31:198-211.

5. Boeddinghaus R, Whyte A. Dental panoramic tomography: an approach for the general radiologist. *Australas Radiol.* 2006;50:526-533.
6. Ludlow JB, Davies-Ludlow LE, White SC. Patient risk related to common dental radiographic examinations: the impact of 2007 International Commission on Radiological Protection recommendations regarding dose calculation. *J Am Dent Assoc.* 2008;139:1237-1243.
7. Bondemark L, Jeppsson M, Lindh-Ingildsen L, Rangne K. Incidental findings of pathology and abnormality in pretreatment orthodontic panoramic radiographs. *Angle Orthod.* 2006;76:98-102.
8. Rushton VE, Horner K, Worthington HV. Screening panoramic radiology of adults in general dental practice: radiological findings. *Br Dent J.* 2001;190:495-501.
9. White SC, Heslop EW, Hollender LG, Mosier KM, Ruprecht A, Shrout MK. Parameters of radiologic care: an official report of the American Academy of Oral and Maxillofacial Radiology. *Oral Surg Oral Med Oral Pathol Oral Radiol Endod.* 2001;91:498-511.
10. Patanachai N, Covavisaruch N, Sinthanayothin C. Wavelet transformation for dental X-ray radiographs segmentation technique, 2010 Eighth International Conference on ICT and Knowledge Engineering, Bangkok, 2010, pp. 103-106, doi:10.1109/ICTKE.2010.5692904.
11. Poonsri A, Aimjirakul N, Charoenpong T, Sukjamsri C. Teeth segmentation from dental x-ray image by template matching, 2016 9th Biomedical Engineering International Conference (BMEiCON), Laung Prabang, 2016, pp. 1-4, doi:10.1109/BMEiCON.2016.7859599.
12. Lira PHM, Giralardi GA, Neves LAP, Feijoo RA. Dental r-ray image segmentation using texture recognition. *IEEE Latin Am Transact.* 2014;12:694-698.
13. Amer YY, Aqel MJ. An efficient segmentation algorithm for panoramic dental images. *Proc Comp Sci.* 2015;65:718-725.
14. Oliveira J, Proença H. *Caries detection in panoramic dental X-ray Images*. Computational Vision and Medical Image Processing. Dordrecht, Germany: Springer Press; 2011:175-190.
15. Hosny A, Parmar C, Quackenbush J, Schwartz LH, Aerts H. Artificial intelligence in radiology. *Nat Rev Cancer.* 2018;18:500-510.
16. Wang S, Summers RM. Machine learning and radiology. *Med Image Anal.* 2012;16:933-951.
17. Beam AL, Kohane IS. Big data and machine learning in health care. *JAMA.* 2018;319:1317-1318.
18. Yeshua T, Mandelbaum YA, Abdalla-Aslan R, et al. Automatic detection and classification of dental restorations in panoramic radiographs. *Issues in Informing Science and Information Technology (IISIT).* 2019;16:221-234. <https://www.informingscience.org/Journals/IISIT/Overview>.
19. Otsu N. A threshold selection method from gray-level histograms. *IEEE Transact Systems Man Cybernet.* 1979;9:62-66.
20. Mohd Khuzi A, Besar R, Wan Zaki W, Ahmad N. Identification of masses in digital mammogram using gray level co-occurrence matrices. *Biomed Imaging Interv J.* 2009;5:e17.
21. Byrne MF, Chapados N, Soudan F, et al. Real-time differentiation of adenomatous and hyperplastic diminutive colorectal polyps during analysis of unaltered videos of standard colonoscopy using a deep learning model. *Gut.* 2019;68:94-100.
22. Xue Y, Zhang R, Deng Y, Chen K, Jiang T. A preliminary examination of the diagnostic value of deep learning in hip osteoarthritis. *PLoS One.* 2017;12.
23. Kindermann J, Leopold E, Paass G. Multi-class classification with error correcting codes. In: Leopold E, Kirsten M, eds. *Technical report, GMD, Oct 2000. Beiträge zum Treffen der GI Fachgruppe 1.1.3 Maschinelles Lernen*, Berlin, Germany: Fraunhofer; 2000. p. 114.
24. McDavid WD, Langlais RP, Welander U, Morris CR. Real, double, and ghost images in rotational panoramic radiography. *Dentomaxillofac Radiol.* 1983;12:122-128.
25. Petersen PE, Kwan S. Evaluation of community-based oral health promotion and oral disease prevention—WHO recommendations for improved evidence in public health practice. *Community Dent Health.* 2004;21:319-329.
26. Vassend O. Anxiety, pain and discomfort associated with dental treatment. *Behav Res Ther.* 1993;31:659-666.
27. Chang HJ, Symkhampha K, Huh KH, et al. The development of a learning management system for dental radiology education: a technical report. *Imaging Sci Dent.* 2017;47:51-55.
28. Heinrich A, Guttler F, Wendt S, et al. Forensic odontology: automatic identification of persons comparing antemortem and post-mortem panoramic radiographs using computer vision. *Rofo.* 2018;190:1152-1158.
29. Rees GV, Woodsend B, Manica S, Revie GF, Brown NL, Mossey PA. Automated Identification from Dental Data (AutoIDD): a new development in digital forensics. *Forensic Sci Int.* 2020;309:110218.

#### Reprint requests:

Chen Nadler  
 Oral Maxillofacial Imaging Unit  
 Oral Medicine Department  
 the Hebrew University  
 Hadassah School of Dental Medicine, Ein Kerem  
 Hadassah Medical Center Jerusalem  
 Israel.  
[Nadler@hadassah.org.il](mailto:Nadler@hadassah.org.il)